Dedicated Dynamic Parameter Identification for Delta-Like Robots

D. Gnad, *Graduate Student Member, IEEE*, H. Gattringer, A. Müller, *Senior Member, IEEE*, W. Höbarth, R. Riepl, and L. Messner

***Abstract*—Dynamics simulation of parallel kinematic manipulators (PKM) and non-linear control methods require a precisely identified dynamics model and explicit generalized mass matrix. Standard methods, which identify so-called dynamic base-parameters, are not sufficient to this end. Algorithms for identifying the complete set of dynamic parameters were proposed for serial manipulators. A dedicated identification method for PKM does not exist, however. Such a method is introduced here for the large class of Delta-like PKM exploiting the parallel structure and making use of model simplifications specific to this class. The proposed method guarantees physical consistency of the identified parameters, and in particular a positive definite generalized mass matrix. The method is applied to a simulated model with exactly known parameters, which allows for verification of the obtained dynamic parameters. The results show that the generalized mass matrix, the acceleration, and the Coriolis, gravitation and friction terms in the equations of motion (EOM) are well approximated. The second example is a real 4-DOF industrial Delta robot ABB IRB 360-6/1600. For this robot, a physically consistent set of inertia and friction parameters is identified from measurements. The method allows prescribing estimated parameters, but does not rely on such data, e.g. from manufacturer or CAD.**

***Index Terms*—Dynamic parameter identification, excitation trajectories, inverse dynamics, mass-inertia parameter identification, model-based control, parallel manipulators.**

I. Introduction

DYNAMICS simulation and advanced model-based non-linear control methods, e.g. computed torque [1] (feedback linearization), passivity based control [2], and augmented PD control [3], rely on equations of motion (EOM) of a robotic manipulator of the form

$$\mathbf{M}(\mathbf{q})\ddot{\mathbf{q}} + \mathbf{C}(\mathbf{q},\dot{\mathbf{q}})\dot{\mathbf{q}} + \mathbf{g}(\mathbf{q}) + \mathbf{f}(\dot{\mathbf{q}}) = \boldsymbol{\tau} \tag{1}$$

where $\mathbf{M}(\mathbf{q})$ is the positive definite generalized mass matrix, $\mathbf{C}(\mathbf{q},\dot{\mathbf{q}})\dot{\mathbf{q}}$ represents Coriolis and centrifugal forces, $\mathbf{g}(\mathbf{q})$ and $\mathbf{f}(\dot{\mathbf{q}})$ are gravitational and friction forces, $\boldsymbol{\tau}$ are actuation forces, and $\mathbf{q}$, $\dot{\mathbf{q}}$, and $\ddot{\mathbf{q}}$ are generalized coordinates, velocity, and acceleration, respectively. Symmetry and positive definiteness of the mass matrix is crucial for forward dynamics simulation, where (1) is solved for $\ddot{\mathbf{q}}$ using Cholesky factorization. Augmented PD control, for instance, additionally requires skew symmetry of $\frac{1}{2}\dot{\mathbf{M}} - \mathbf{C}$. Symmetry and positive definiteness of the mass matrix are guaranteed only if the inertia parameters of each (rigid) body of the system is physically consistent. This requirement is not taken into account by standard identification methods. Standard identification methods identify dynamic parameters, summarized in $\mathbf{p}$, of an inverse dynamics model

$$\boldsymbol{\tau} = \mathbf{Y}(\mathbf{q},\dot{\mathbf{q}},\ddot{\mathbf{q}})\,\mathbf{p} \tag{2}$$

exploiting the fact that the EOM (1) are linear in the inertia and (standard) friction parameters [4]. However, not all dynamic parameters in $\mathbf{p}$ can be identified since (2) does not have a unique solution. A solution is given in terms of linear combinations of the inertia parameters, referred to as base-parameters. The base-parameters are obtained as a least squares solution without conditions on physical consistency. This approach was introduced for serial robots [4], and later for parallel robots [5], [6]. Identification of base-parameters leads to an inverse dynamics model that allows for computing the feed-forward control $\boldsymbol{\tau}$ for given motion $\mathbf{q}(t)$, but it does not yield explicit EOM of the form (1).

The inertia properties of a rigid body are physically consistent if they satisfy the following three conditions: the mass m is positive, the inertia tensor $\boldsymbol{\Theta}$ is positive definite, and the moments of inertia satisfy the so-called triangle inequalities. The base-parameter identification does not account for these conditions, and often leads to physical inconsistencies [7], [8]. To ensure consistency, the above three conditions were included as linear matrix inequality constraints [9], [10], [11], [12]. An unconstrained formulation that ensures physical consistency was proposed in [13] by means of a non-linear transformation of the dynamic parameters to another set of algorithmic parameters.

Up to now, identification of physically consistent inertia parameters has exclusively been pursued for serial kinematic robots. This paper, for the first time in the literature, presents a method to identify physically consistent dynamics parameters of Delta-like robots. The method is suited for various robots belonging to that class of PKM and demonstrated using the 4 DOF Delta robot. The kinematic structure of the PKM is exploited to simplify the model, speed up the computation time, and improve the identification result. The presented method provides a foundation for applications that require explicit models, e. g. forward dynamics simulation, model-based control schemes,

Manuscript received 16 February 2024; accepted 12 March 2024. Date of publication 22 March 2024; date of current version 2 April 2024. This letter was recommended for publication by Associate Editor L. Biagiotti and Editor L. Pallottino upon evaluation of the reviewers' comments. This work was supported by the LCM K2 Center for Symbiotic Mechatronics within the framework of the Austrian COMET-K2 Program. *(Corresponding author: Daniel Gnad.)*

D. Gnad, H. Gattringer, and A. Müller are with the Institute of Robotics, Johannes Kepler University Linz, 4040 Linz, Austria (e-mail: daniel.gnad@jku.at; hubert.gattringer@jku.at; a.mueller@jku.at).

W. Höbarth, R. Riepl, and L. Messner are with B&R Industrial Automation, 5142 Eggelsberg, Austria (e-mail: wolfgang.hoebarth@br-automation.com; roland.riepl@br-automation.com; lukas.messner@br-automation.com).

Digital Object Identifier 10.1109/LRA.2024.3380924

and constraint force computation. The method does not need additional information, e.g. CAD data from robot manufacturers.

II. Existing Approaches to Dynamics Modeling

A. Delta-Like Robots

High-speed applications and design of Delta robots necessitate model-based control schemes and dynamics simulations, thus on correct dynamics parameters. There are various other PKM designs that all share the same principle setup, in the following referred to as *Delta-like* robots [14]. A Delta-like manipulator is understood to be a PKM where each limb, connecting moving platform and base, consists of an articulated link (called upper arm or shoulder) followed by a parallelogram mechanism formed by two slender struts. For example, Clavel's original 3 DOF Delta robot [15] comprises three limbs where the first link is connected to the base by an actuated revolute joint (R-joint), and the two struts of the parallelogram are connected by R-joints. The platform can perform spatial translations. The 4 DOF version of the Delta contains an additional telescope bar Cardanically suspended between base and platform at which the end-effector (EE) is attached. In most of the industrially available Delta robots, a spherical joint (S-joint) is used instead of the two R-joints connecting the struts. These S-joints are formed by a ball and a (partially cut) socket held together with springs. This is kinematically equivalent to two subsequent R-joints. Various variations with different actuation and DOF were proposed. The H4 [16], I4 [17], and Par4 [18] are examples with 4 DOF, which contain an articulated platform to generate platform rotations about a constant axis, and can be actuated by revolute or linear actuators. The particular kinematic structure of Delta-like robots can be exploited for deriving a tailored inverse dynamics model with a reduced set of dynamic parameters.

B. Model Simplification

All identification schemes so far, especially for the family of Delta-like robots, share some similarities in terms of model simplifications. Due to the lightweight structure of the arms and struts, the slender struts (also called 'forearms') are often regarded as point-masses located at the end of the upper arm [6], [19]. In [14], [20], [21] half of the mass of a strut is added to the end of the upper arm and to the moving platform, respectively. In [19] it is assumed that the center of mass (COM) of the upper arm is at the geometric center. The common assumption of the above references is that all upper arms and all struts are identical and can consequently be described by the same inertia parameters. This implies a drastic reduction of the unknown inertia parameters. There are even further simplifications especially w.r.t. the slender struts introduced in the literature. Some approaches even neglected the mass of the struts, and hence all inertia effects of the struts [22], [23]. Various other (non Delta-like) PKMs [24] were also described in terms of base-parameters [25], [26]. However, none of these account for physical consistency of the inertia and friction parameters. Additionally, [20], [27] further rely on CAD data available for the identification scheme.

III. Inverse Dynamics Model

The inverse dynamics model is expressed in terms of the complete set of dynamic parameters.

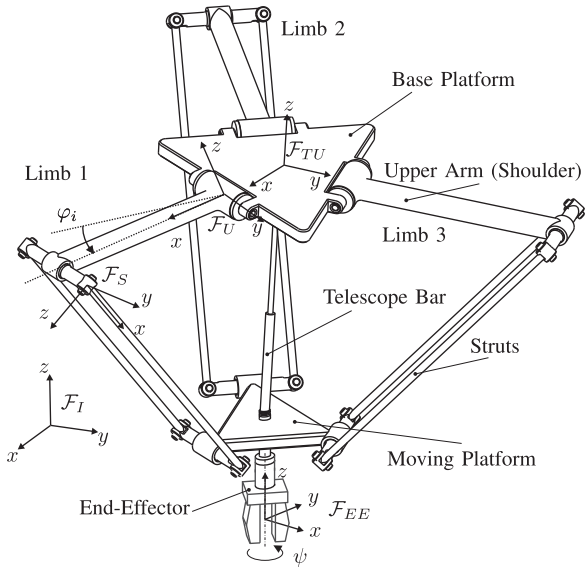

Fig. 1. Sketch of the $\delta = 4$ DOF Delta model kinematically equivalent to the ABB IRB 360-6/1600 treated as example in Section VIII. The telescope bar is often also referred to as Cardanic axle or spindle.

A. Inverse Kinematics

The Delta robot in Fig. 1 is used as representative example throughout the paper. Its motion is described by the $\delta = 4$ actuator coordinates $\mathbf{q}^\mathsf{T} = [\varphi_1 \quad \varphi_2 \quad \varphi_3 \quad \psi]$, which serve as generalized coordinates, where φ_i denotes the angle of the actuated R-joint connecting the shoulder of limb $i = 1, 2, 3$ to the base, and ψ is the rotation angle of the actuated universal joint of the vertical telescope bar. The EE pose is described by the task space coordinates $\mathbf{z}^\mathsf{T} = [{}_I\mathbf{r}^\mathsf{T} \quad \psi]$, where ${}_I\mathbf{r}$ is the position vector of the platform, resolved in inertial frame $\mathcal{F}_I$, and the rotation of the EE is identical to the rotation angle ψ of the telescope bar drive. The actuator coordinates are determined by the task space coordinates via the inverse kinematics map $\mathbf{q} = \mathbf{f}_{\text{IK}}(\mathbf{z})$.

B. Equations of Motion in Parameter-Linear Form

As the forward kinematics $\mathbf{z} = \mathbf{f}_{\text{FK}}(\mathbf{q})$ can (locally) be solved analytically, the EOM of a Delta-like robot can be expressed in the general form (1).

The EOM are linear in the dynamic parameters. If the PKM contains N moving bodies and n_f joints where viscous and Coulomb friction are considered, the inverse dynamics model can be written in the parameter-linear form (2) with

$$\mathbf{Y}(\mathbf{q}, \dot{\mathbf{q}}, \ddot{\mathbf{q}})\, \mathbf{p} = \sum_{i=1}^{N} \mathbf{Y}_i(\mathbf{q}, \dot{\mathbf{q}}, \ddot{\mathbf{q}})\, \mathbf{p}_i + \mathbf{Y}_\text{f}(\mathbf{q}, \dot{\mathbf{q}})\, \mathbf{p}_\text{f} \tag{3}$$

where $\mathbf{Y} = [\mathbf{Y}_1, \ldots, \mathbf{Y}_N, \mathbf{Y}_\text{f}]$ is a $\delta \times (10N + 2n_\text{f})$ matrix, and

$$\mathbf{p}_i = \begin{bmatrix} m & m\,\mathbf{c}^\mathsf{T} & \Theta_{xx} & \Theta_{yy} & \Theta_{zz} & \Theta_{xy} & \Theta_{yz} & \Theta_{xz} \end{bmatrix}_i^\mathsf{T} \tag{4}$$

comprises the 10 inertia parameters of body i. Therein, m is the mass, and $\mathbf{c} = [c_x \quad c_y, \quad c_z]^\mathsf{T}$ the position vector of the COM measured from the joint (or link) frame, so that $m\mathbf{c}$ comprises

the first moments of inertia. The symmetric inertia tensor

$$\boldsymbol{\Theta} = \begin{bmatrix} \Theta_{xx} & \Theta_{xy} & \Theta_{xz} \\ \Theta_{xy} & \Theta_{yy} & \Theta_{yz} \\ \Theta_{xz} & \Theta_{yz} & \Theta_{zz} \end{bmatrix} \tag{5}$$

comprises the second moments of inertia w.r.t. the joint frame. The $\delta \times 2n_\mathrm{f}$ matrix $\mathbf{Y}_\mathrm{f} = [\mathbf{Y}_\mathrm{v} \quad \mathbf{Y}_\mathrm{c}]$ in combination with the friction parameter vector $\mathbf{p}_\mathrm{f}^\mathsf{T} = [\mathbf{p}_\mathrm{v}^\mathsf{T} \quad \mathbf{p}_\mathrm{c}^\mathsf{T}]$ yields generalized forces $\mathbf{Y}_\mathrm{v}\mathbf{p}_\mathrm{v}$ due to viscous friction and $\mathbf{Y}_\mathrm{c}\mathbf{p}_\mathrm{c}$ due to Coulomb friction. For the viscous friction forces, the matrix

$$\mathbf{Y}_\mathrm{v} = \begin{bmatrix} \mathrm{diag}(\dot{\mathbf{q}}) & \left(\dot{\vartheta}_j \frac{\partial \dot{\vartheta}_j}{\partial \dot{\mathbf{q}}}\right)^\mathsf{T}_{j=1\ldots n_\mathrm{f}-\delta} \end{bmatrix} \tag{6}$$

contains a diagonal matrix of the velocities of the (actuated) coordinates $\mathrm{diag}(\dot{\mathbf{q}})$ and partial derivatives of velocities $\dot{\vartheta}_1, \ldots, \dot{\vartheta}_{n_\mathrm{f}-\delta}$ of further joints whose friction is modeled. The viscous friction parameter vector $\mathbf{p}_\mathrm{v} = [p_{\mathrm{v}_1}, \ldots p_{\mathrm{v}_{n_\mathrm{f}}}]$ contains the viscous friction coefficients. Analogously, Coulomb friction is described with

$$\mathbf{Y}_\mathrm{c} = \begin{bmatrix} \mathrm{diag}(\mathrm{sign}(\dot{\mathbf{q}})) & \left(\mathrm{sign}(\dot{\vartheta}_j) \frac{\partial \dot{\vartheta}_j}{\partial \dot{\mathbf{q}}}\right)^\mathsf{T}_{j=1\ldots n_\mathrm{f}-\delta} \end{bmatrix} \tag{7}$$

where $\mathbf{p}_\mathrm{c} = [p_{\mathrm{c}_i}, \ldots, p_{\mathrm{c}_{n_\mathrm{f}}}]$ comprises the Coulomb friction coefficients. The parameter vector $\mathbf{p}^\mathsf{T} = [\mathbf{p}_i^\mathsf{T}, i = 1 \ldots N \quad \mathbf{p}_\mathrm{f}^\mathsf{T}]$ comprises the total $10\,N$ inertia and $2n_\mathrm{f}$ friction parameters.

IV. Persistent Excitation Trajectory

Trajectories are determined that yield a persistent excitation for identification of base-parameters. It is assumed that these are also valid trajectories for identification of the full set of parameters $\mathbf{p}$.

A. Determination of Independent Base-Parameters

The matrix $\mathbf{Y}(\mathbf{q}, \dot{\mathbf{q}}, \ddot{\mathbf{q}})$ is evaluated for ν different realizations of $(\mathbf{q}, \dot{\mathbf{q}}, \ddot{\mathbf{q}})$, with $\nu \geq (10N + 2n_\mathrm{f})/\delta$. The obtained matrices are stacked to form a $\nu\delta \times (10N + 2n_\mathrm{f})$ matrix $\bar{\mathbf{Y}}$, called the system regressor matrix. Not all of the $(10N + 2n_\mathrm{f})$ parameters in $\mathbf{p}$ are identifiable, thus the maximal rank of $\bar{\mathbf{Y}}$ is $\nu_\mathrm{B} < (10N + 2n_\mathrm{f})$. A QR factorization $\bar{\mathbf{Y}} = \mathbf{QR}$ is used to identify ν_B linearly independent columns, indicated by the values on the main diagonal of $\mathbf{R}$, which gives rise to a $\nu\delta \times \nu_\mathrm{B}$ matrix $\bar{\mathbf{Y}}_\mathrm{B}$.

The conditioning of the reduced matrix $\bar{\mathbf{Y}}_\mathrm{B}$ depends on the realizations $\mathbf{q}, \dot{\mathbf{q}}, \ddot{\mathbf{q}}$ at which $\mathbf{Y}$ is evaluated. For serial manipulators, uniform sampling of $\mathbf{q}, \dot{\mathbf{q}}, \ddot{\mathbf{q}}$, within the joint limits, can be pursued to obtain representative samples. For PKM, due to the loop constraints, the admissible range joint coordinates and derivatives is defined by nonlinear relations depending on the joint limits, which makes a uniform sampling in joints space difficult. Instead, a random sampling can be pursued in task space. To this end, task space coordinates $\mathbf{z}$ are restricted to an approximated workspace, and joint variables are computed from the inverse kinematics $\mathbf{q} = \mathbf{f}_\mathrm{IK}(\mathbf{z})$. The task space boundary can usually be approximated easily. This is shown in Fig. 2 for the industrial Delta robot ABB IRB 360-6/1600 used as example in Section VIII, where it is approximated by a hemisphere $\mathcal{B}$.

The realizations of the motor torques are summarized in vector $\bar{\boldsymbol{\tau}}$. This gives rise to the linear regression problem $\bar{\boldsymbol{\tau}} = \bar{\mathbf{Y}}_\mathrm{B}\mathbf{p}_\mathrm{B}$, where $\mathbf{p}_\mathrm{B}$ is a vector of ν_B base-parameters, and $\bar{\mathbf{Y}}_\mathrm{B}$ serves as

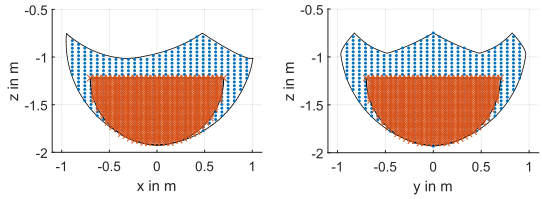

Fig. 2. Approximation of the task space (blue dotted texture) of the industrial Delta robot ABB IRB 360-6/1600 with a hemisphere $\mathcal{B}$ approximation (orange and more dense pattern).

regressor matrix. Identification of base-parameters thus boils down to solving the linear regression problem for recorded motion and corresponding actuation torques. The rank of $\bar{\mathbf{Y}}_\mathrm{B}$ is ν_B, and the regression problem has a unique solution. The solution minimizing the weighted squared error $\|\bar{\boldsymbol{\tau}} - \bar{\mathbf{Y}}_\mathrm{B}\mathbf{p}_\mathrm{B}\|^2_{\mathbf{W}_{\boldsymbol{\tau}}}$ is $\mathbf{p}_\mathrm{B} = (\bar{\mathbf{Y}}_\mathrm{B}^\mathsf{T}\mathbf{W}_{\boldsymbol{\tau}}\bar{\mathbf{Y}}_\mathrm{B})^{-1}\bar{\mathbf{Y}}_\mathrm{B}^\mathsf{T}\mathbf{W}_{\boldsymbol{\tau}}\bar{\boldsymbol{\tau}}$. Therein, and throughout the paper $\|\mathbf{x}\|_\mathbf{W} = \sqrt{\mathbf{x}^\mathsf{T}\mathbf{W}\mathbf{x}}$ denotes weighted norm of a vector $\mathbf{x}$ w.r.t. a metric $\mathbf{W}$. If $\mathbf{W}_{\boldsymbol{\tau}} = \boldsymbol{\Sigma}^{-1}$ is used, where $\boldsymbol{\Sigma}$ is the covariance matrix of the actuation torques $\boldsymbol{\tau}$ derived from the motor torque measurements, then this is an unbiased minimum variance Gauss-Markov estimator [28], [29]. However, in order to obtain $\boldsymbol{\Sigma}$, an estimator for the motor torques $\boldsymbol{\tau}$, i.e. an identified model, is needed beforehand. If available, estimated base-parameters can be used to obtain an estimate for $\boldsymbol{\Sigma}$ [28]. In the following the weight $\mathbf{W}_{\boldsymbol{\tau}} = \mathrm{diag}(\boldsymbol{\tau}_\mathrm{max})^{-2}$ will be used, where elements of $\boldsymbol{\tau}_\mathrm{max}$ are the maximal values of the respective drive torque, which yields a dimensionless normalization of the torques $\boldsymbol{\tau}$.

B. Trajectory Optimization

The regressor matrix serves to determine optimal identification trajectories. Trajectories are determined such that $\bar{\mathbf{Y}}_\mathrm{B}$ is well-conditioned, and thus lead to persistent excitation.

In case of PKM, the motion is best described in task space. To this end, the task space trajectory $\mathbf{z}(t)$ (EE translation and rotation about the vertical axis) is expressed as truncated Fourier series [30]

$$z_i = b_{i,0} + \sum_{k=1}^{n_F} [a_{i,k}\sin(\omega_0 k t) + b_{i,k}\cos(\omega_0 k t)] \tag{8}$$

with base frequency ω_0. The coefficients $a_{i,k}$ and $b_{i,k}$ are determined so to produce a persistent excitation of all base-parameters [31]. Persistency is reflected by the conditioning of the regressor matrix $\bar{\mathbf{Y}}_\mathrm{B}$. This is quantified by the index $J := \mathrm{cond}(\bar{\mathbf{Y}}_\mathrm{B}^\mathsf{T}\bar{\mathbf{Y}}_\mathrm{B})$ or $J := -\det(\bar{\mathbf{Y}}_\mathrm{B}^\mathsf{T}\bar{\mathbf{Y}}_\mathrm{B})$. An overview of the suitable objective functions for computing optimal excitation trajectories was reported in [32], along with interpretations of the associated Fischer-Information [29]. The coefficients $\mathbf{a}_i = [a_{i,1} \quad \ldots \quad a_{i,n_F}]$, $\mathbf{b}_i = [b_{i,0} \quad \ldots \quad b_{i,n_F}]$ and the base frequency ω_0 are determined by solving the optimization problem

$$\min_{\mathbf{a},\mathbf{b},\omega_0} \quad \left(J - w\|\dot{\mathbf{q}}\|_{\mathbf{W}_{\dot{\mathbf{q}}}}\right) \tag{9}$$

$$\text{s.t. } {}_I\mathbf{r} \in \mathcal{B}, \qquad |\dot{\mathbf{z}}| \leq \dot{\mathbf{z}}_\mathrm{max}, \quad |\ddot{\mathbf{z}}| \leq \ddot{\mathbf{z}}_\mathrm{max}, \tag{10}$$

$$\mathbf{q}_\mathrm{min} \leq \mathbf{q} \leq \mathbf{q}_\mathrm{max}, \; |\dot{\mathbf{q}}| \leq \dot{\mathbf{q}}_\mathrm{max}, \quad |\ddot{\mathbf{q}}| \leq \ddot{\mathbf{q}}_\mathrm{max}, \tag{11}$$

where $\mathcal{B} \in \mathbb{R}^3$ is the admissible range of the position vector ${}_I\mathbf{r}$, as part of the task space coordinates $\mathbf{z}$, and $\dot{\mathbf{z}}_{\max}, \ddot{\mathbf{z}}_{\max}$ are the upper limits of the derivatives of task space coordinates. Furthermore, $\mathbf{q}_{\min}, \mathbf{q}_{\max}$ are limits of joint coordinates, and $\dot{\mathbf{q}}_{\max}, \ddot{\mathbf{q}}_{\max}$ of the velocities and accelerations, respectively. The second term in (9) is included to aid the identification of friction. In this term, the joint velocities $\dot{\mathbf{q}}$ are normalized using the weighting matrix $\mathbf{W}_{\dot{\mathbf{q}}} = \operatorname{diag}(\dot{\mathbf{q}}_{\max})^{-2}$, and the scaling factor w is used to ensure sufficiently high velocities. Notice that no explicit collision avoidance constraints are necessary since the EE position is confined to ${}_I\mathbf{r} \in \mathcal{B}$, which is sufficient for Delta-like robot.

V. Identification of Physically Consistent Dynamic Parameters

A. Transformation of Inertia Parameters

The conditions on the inertia data of rigid body i can be expressed by means of the 4×4 inertia matrix, which was introduced in multibody dynamics in [33],

$$\bar{\mathsf{M}}_i(\mathbf{p}_i) = \begin{bmatrix} \bar{\boldsymbol{\Theta}}_i & m_i \mathbf{c}_i \\ m_i \mathbf{c}_i^{\mathsf{T}} & m_i \end{bmatrix} \tag{12}$$

where $\bar{\boldsymbol{\Theta}}_i = \frac{1}{2}\operatorname{tr}(\boldsymbol{\Theta}_i)\mathbf{I} - \boldsymbol{\Theta}_i$ is Binet's inertia tensor [34]. The 10 inertia parameters $\mathbf{p}_i$ are physically consistent if and only if $\bar{\mathsf{M}}_i(\mathbf{p}_i)$ is positive definite [11]. This obviously implies positiveness of the mass m, while positiveness of $\bar{\boldsymbol{\Theta}}_i$ accounts for the triangle inequalities $\lambda_a + \lambda_b > \lambda_c; a, b, c \in \{1, 2, 3\}$, with the eigenvalues $\lambda_1, \lambda_2, \lambda_3$ of the inertia tensor $\boldsymbol{\Theta}_i$ in (5). If $\boldsymbol{\Theta}_i$ is expressed in a principle axis frame, the eigenvalues correspond to the principal inertia moments.

Being positive definite, matrix (12) possesses a Cholesky factorization $\bar{\mathsf{M}}_i = \mathbf{U}^{\mathsf{T}}\mathbf{U}$, with an upper triangular matrix $\mathbf{U}$ (omitting index i). Requiring the diagonal elements of $\mathbf{U}(\boldsymbol{\pi}_i)$ to be positive ensures positive definiteness of $\bar{\mathsf{M}}_i$. This requirement is imposed by introducing another set of 10 parameters

$$\boldsymbol{\pi}_i^{\mathsf{T}} = [\alpha \quad d_1 \quad d_2 \quad d_3 \quad s_{12} \quad s_{23} \quad s_{13} \quad t_1 \quad t_2 \quad t_3] \tag{13}$$

to parameterize $\mathbf{U}(\boldsymbol{\pi}_i)$, which leads to the log-Cholesky factorization $\bar{\mathsf{M}}_i(\boldsymbol{\pi}_i) = \mathbf{U}^{\mathsf{T}}(\boldsymbol{\pi}_i)\mathbf{U}(\boldsymbol{\pi}_i)$, as proposed in [13]. Comparing elements of $\bar{\mathsf{M}}(\mathbf{p}_i)$ and $\bar{\mathsf{M}}_i(\boldsymbol{\pi}_i)$ yields the relation

$$\begin{aligned} \mathbf{p}_i(\boldsymbol{\pi}_i) = \mathrm{e}^{2\alpha}[&t_1^2 + t_2^2 + t_3^2 + 1,\ t_1\,\mathrm{e}^{d_1},\ t_1\,s_{12} + t_2\,\mathrm{e}^{d_2}, \\ &t_1\,s_{13} + t_2\,s_{23} + t_3\,\mathrm{e}^{d_3}, \\ &s_{12}^2 + s_{23}^2 + s_{13}^2 + \mathrm{e}^{2d_2} + \mathrm{e}^{2d_3}, \\ &s_{12}^2 + s_{13}^2 + \mathrm{e}^{2d_1} + \mathrm{e}^{2d_3},\ -s_{12}\,\mathrm{e}^{d_1}, \\ &-s_{12}\,s_{13} - s_{23}\,\mathrm{e}^{d_2},\ -s_{13}\,\mathrm{e}^{d_1}] \end{aligned} \tag{14}$$

of the original physical parameters $\mathbf{p}_i$ and the new parameter set $\boldsymbol{\pi}_i$. The elements in $\boldsymbol{\pi}_i$ can be physically interpreted as deformation of a reference body in order to achieve the desired inertia [13]. This parameterization ensures the positive definiteness of the inertia matrix $\boldsymbol{\Theta}_i$ and consequently all necessary conditions for a physically meaningful body, hence the resulting parameter vector $\mathbf{p}_i(\boldsymbol{\pi}_i)$ is physically consistent.

It is important to notice that the above parameterization (14) ensures that for any choice of $\boldsymbol{\pi}_i$ the inertia parameter $\mathbf{p}_i(\boldsymbol{\pi}_i)$ is physically feasible. As a consequence, it is not possible to omit principle moments of inertia $\Theta_{xx}, \Theta_{yy}, \Theta_{zz}$, which would lead to a physically infeasible body. This must be taken into account when some of these inertia moments do not appear in the EOM, and would not need to be identified (see Section VI).

B. Transformation of Friction Parameters

The only constraint on the viscous friction parameters $\mathbf{p}_{\mathrm{v}}$ and the Coulomb friction coefficients $\mathbf{p}_{\mathrm{c}}$ to be physically consistent, is that each of these coefficients must be positive. This is ensured by the transformation $p_{\mathrm{v}_i} = \mathrm{e}^{\beta_i}, p_{\mathrm{c}_i} = \mathrm{e}^{\sigma_i}, i = 1 \ldots n_{\mathrm{f}}$ to a new set of friction parameters $\boldsymbol{\pi}_{\mathrm{f}}^{\mathsf{T}} = [\beta_1 \quad \ldots \quad \beta_{n_{\mathrm{f}}} \quad \sigma_1 \quad \ldots \quad \sigma_{n_{\mathrm{f}}}]$. The original friction coefficients $\mathbf{p}_{\mathrm{f}}(\boldsymbol{\pi}_{\mathrm{f}})$ are thus always positive for any $\boldsymbol{\pi}_{\mathrm{f}}$.

C. Determination of Complete Set of Parameters

The overall vector of $10N + 2n_{\mathrm{f}}$ original and transformed inertia and friction parameters is denoted $\mathbf{p}^{\mathsf{T}} = [\mathbf{p}_{\mathrm{I}}^{\mathsf{T}} \quad \mathbf{p}_{\mathrm{f}}^{\mathsf{T}}]$ and $\boldsymbol{\pi}^{\mathsf{T}} = [\boldsymbol{\pi}_{\mathrm{I}}^{\mathsf{T}} \quad \boldsymbol{\pi}_{\mathrm{f}}^{\mathsf{T}}]$, respectively. The persistent excitation trajectory is executed and s samples are recorded for $\mathbf{q}, \dot{\mathbf{q}}, \ddot{\mathbf{q}} \in \mathbb{R}^{\delta}$ and for the actuation torques $\boldsymbol{\tau} \in \mathbb{R}^{\delta}$. Denote with $\bar{\boldsymbol{\tau}} \in \mathbb{R}^{s\delta}$ the vector comprising the recorded torque values, and with $\bar{\mathbf{Y}}$ the $s\delta \times (10N + 2n_{\mathrm{f}})$ matrix formed by stacking the matrix $\mathbf{Y}$ evaluated at the s samples. Identifying the inertia and friction parameters amounts to find $\boldsymbol{\pi}$ minimizing the error $\|\bar{\boldsymbol{\tau}} - \bar{\mathbf{Y}}\mathbf{p}(\boldsymbol{\pi})\|^2_{\mathbf{W}_{\boldsymbol{\tau}}}$, where $\mathbf{W}_{\boldsymbol{\tau}} = \operatorname{diag}(\bar{\boldsymbol{\tau}}_{\max})^{-2}$ is used to normalize and homogenize the error. The system regressor matrix is not full rank, since not all dynamic parameters can be identified, and there is no unique solution $\boldsymbol{\pi}$ minimizing this error. Therefore, a regularization is needed.

To this end, nominal or estimated parameter values $\mathbf{p}_{\mathrm{reg}}$ are prescribed and the objective function

$$J(\boldsymbol{\pi}) := \frac{\gamma_{\boldsymbol{\tau}}}{s}\left\|\bar{\boldsymbol{\tau}} - \bar{\mathbf{Y}}\mathbf{p}(\boldsymbol{\pi})\right\|^2_{\mathbf{W}_{\boldsymbol{\tau}}} + \gamma_{\mathbf{p}}\left\|\mathbf{p}(\boldsymbol{\pi}) - \mathbf{p}_{\mathrm{reg}}\right\|^2_{\mathbf{W}_{\mathbf{p}}} \tag{15}$$

is introduced, where $\mathbf{W}_{\mathbf{p}} = \operatorname{diag}(\mathbf{p}_{\mathrm{reg}})^{-2}$, and $\gamma_{\boldsymbol{\tau}}, \gamma_{\mathbf{p}} \in \mathbb{R}_+$ are weighting coefficients. The identification problem amounts to find parameters $\boldsymbol{\pi}$ minimizing $J(\boldsymbol{\pi})$. The additional second term serves as regularization term. The smaller the ratio $\gamma_{\boldsymbol{\tau}}/\gamma_{\mathbf{p}}$ the closer the computed parameter are to the regularization term $\mathbf{p}_{\mathrm{reg}}$. The latter also provides a means to prescribe physically consistent initial values for numerically minimizing the objective (15). It is to be noticed that the value $\boldsymbol{\pi}^*$ is uniquely related to $\mathbf{p}^*$ at which the objective (15) attains the minimum. With the weights $\mathbf{W}_{\boldsymbol{\tau}}$ and $\mathbf{W}_{\mathbf{p}}$, the objective function (15) is dimensionless, and the second term is the relative difference of the current parameter value and the regularization term. The latter term could, alternatively be replaced by a measure of difference of the inertia matrix (12) obtained with either parameter vector. This was proposed in [35], [36], where a matrix norm $d(\bar{\mathsf{M}}(\mathbf{p}), \bar{\mathsf{M}}(\mathbf{p}_{\mathrm{reg}}))$ was used.

VI. Parameter Reduction for Delta-Like Robots

Delta-like robots possess very special kinematics and geometric proportions. This fact allows for neglecting certain dynamic parameters a priori.

a) Deviation moments: Since the principal geometric extensions of the links are generally known, the link frames are

assumed to be aligned with the principal axis of inertia. Thus, as first simplification the deviation moments $\Theta_{xy}, \Theta_{yz}, \Theta_{xz}$ are set to zero. This implies $s_{12} = s_{23} = s_{13} = 0$, and leads to the reduced parameter vector

$$\mathbf{p}_i(\boldsymbol{\pi}_i) = \mathrm{e}^{2\alpha}\left[t_1^2 + t_2^2 + t_3^2 + 1,\ t_1\,\mathrm{e}^{d_1},\ t_2\,\mathrm{e}^{d_2},\ t_3\,\mathrm{e}^{d_3},\right.$$
$$\left.\mathrm{e}^{2d_2} + \mathrm{e}^{2d_3},\ \mathrm{e}^{2d_1} + \mathrm{e}^{2d_3},\ \mathrm{e}^{2d_1} + \mathrm{e}^{2d_2}\right]. \quad (16)$$

b) Upper arms (shoulder): The upper arms only execute a rotary motion about the y-axis of the link frame $\mathcal{F}_U$, as shown in Fig. 1. Hence, only the first mass-moments $m\,c_x, m\,c_z$, and the principal inertia moment Θ_{yy} contribute to the EOM, and thus to the motor torques $\boldsymbol{\tau}$. The first mass moment $m\,c_y = 0$ can be set to zero, resulting in $t_2 = 0$, and the remaining principle inertia moments can be neglected. Consequently, it is sufficient to use the reduced inertia parameter vector $\mathbf{p}_U(\boldsymbol{\pi}_U) = [m \quad mc_x \quad mc_z \quad \Theta_{yy}]^\mathsf{T}$ which is described by the four parameters in $\boldsymbol{\pi}_U = [d_1 \quad d_3 \quad t_1 \quad t_3]^\mathsf{T}$. This reduction does not change the EOM.

c) Lower arms (parallelogram formed by slender struts): The QR factorization of the regressor matrix indicates that all 10 parameters can be identified. The values range from 0.4 associated with the rotatory inertia up to 104 representing the mass. However, for feasible motions of the Delta, the inertia effects due to the first mass moments $m\,c_y$ and $m\,c_z$ (lateral motions of the strut according to link frame $\mathcal{F}_S$ shown in Fig. 1), and due to the longitudinal inertia Θ_{xx} (rotation about the beam axis) are not sufficiently excited for reliable identification, thus have insignificant contributions to the mass matrix. This is confirmed by the corresponding small value in the QR-decomposition. A simplification for the struts is thus to set the first mass moments $m\,c_y = m\,c_z = 0$ and thus with (16) directly yields $t_2 = t_3 = 0$. The only remaining non-zero parameters in (13) are $\boldsymbol{\pi}_\mathrm{S} = [\alpha \quad d_1 \quad d_2 \quad d_3 \quad t_1]^\mathsf{T}$ with the corresponding parameter vector $\mathbf{p}_S(\boldsymbol{\pi}_S)$. Note that although simplifications were made, the longitudinal inertia Θ_{xx} cannot be set to zero, due to the properties of the mapping (14), discussed in Section V-A.

d) Telescope bar: The telescope bar consists of an upper and a lower part that are connected by a prismatic joint. The upper part is connected to the base via a universal joint, and the lower part by a universal joint to the moving platform. The link frame $\mathcal{F}_{TU}$ (see Fig. 1) is located at the center of the universal joint at the upper part. Its z axis is aligned with the prismatic joint. Both parts of the telescope bar are rotatory symmetrical, thus the COM of the two parts is assumed to be located along the respective symmetry axis. Therewith, the first order moments vanish $m\,c_x = m\,c_y = 0$, and thus $t_1 = t_2 = 0$. The QR factorization shows that all parameters of the lower part of the telescope bar can be identified. It further indicates that the mass m of the upper part cannot be identified separately as the upper part tilts and rotates about the universal joint at the base, but does not translate independently. Since a nominal value of the mass of the upper part can usually be estimated (see Section VIII), it is kept as a parameter, which serves as regularization term. The remaining non-zero parameters for the upper and lower part are $\mathbf{p}_{TU}(\boldsymbol{\pi}_{TU}) = [m \quad mc_z \quad \Theta_{xx} \quad \Theta_{yy} \quad \Theta_{zz}]^\mathsf{T}$ and $\mathbf{p}_{TL}(\boldsymbol{\pi}_{TL}) = [m \quad mc_z \quad \Theta_{xx} \quad \Theta_{yy} \quad \Theta_{zz}]^\mathsf{T}$, respectively, which translates into the transformed parameters $\boldsymbol{\pi}_{TU} = [\alpha \quad d_1 \quad d_2 \quad d_3 \quad t_3]^\mathsf{T}$ and $\boldsymbol{\pi}_{TL} = [\alpha \quad d_1 \quad d_2 \quad d_3 \quad t_3]^\mathsf{T}$.

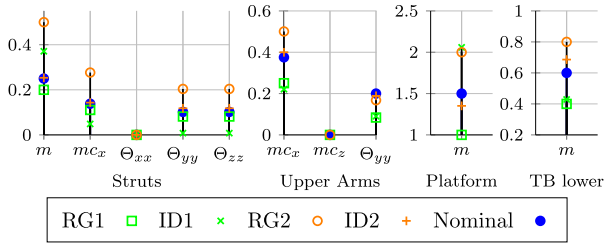

Fig. 3. Comparison of identified parameter $\mathbf{p}$ for two different regularization values. The longitudinal inertia Θ_{xx} of the struts is still parameterized by the non-linear mapping and always greater than zero.

e) Platform: The platform of the Delta only performs translational motions, hence only the mass of the platform can be identified, resulting in $\boldsymbol{\pi}_P = [\alpha]$ with $\mathbf{p}_P(\boldsymbol{\pi}_P)$.

f) End-Effector: For the EE, with the joint frame $\mathcal{F}_{EE}$ shown in Fig. 1, the mass m, first mass-moments $m\,c_x, m\,c_y$ together with the rotatory inertia Θ_{zz} can be identified according to the QR factorization. Hence, for the EE $\boldsymbol{\pi}_{EE} = [\alpha \quad d_1 \quad d_2 \quad t_1 \quad t_2]^\mathsf{T}$ with $\mathbf{p}_{EE}(\boldsymbol{\pi}_{EE})$ can be used. However, usually the EE can be assumed to be known, since most of the time for the mounted tool CAD data is available, which can be used as regularization parameter. In this case the EE can be assumed to be known and excluded from the identification.

g) Parallel Topology: Delta-like robots are fully parallel manipulators, and the several limbs are usually constructed with identical geometric and dynamic parameters. This is exploited for the identification, and the same (updated) parameters are used for the three limbs. This is also advantageous for the performance of the identification since the effect of the individual parameters on the actuation torques is increased.

In summary, with the above simplifications, only 36 optimization variables are necessary to parameterize the rigid bodies and the friction coefficients, whereas 61 parameters would be necessary if all rigid bodies were fully parameterized. When using the reduced set of independent dynamic parameters, 37 base-parameters are required, which are not guaranteed to be physically consistent, however.

VII. Example 1: Identification of Surrogate Test Model

The proposed method is first applied to identify a simulation model of the 4 DOF Delta. That is, all inertia parameters and friction parameters to be identified are known exactly, which are referred to as nominal parameters. Viscous and Coulomb friction is modeled in the actuated joints and the prismatic joint of the telescope bar. The simulation model was implemented in Matlab with assumed nominal parameters. The minimization problem $\min_{\boldsymbol{\pi}} J(\boldsymbol{\pi})$ with J in (15) was solved with the optimization library Yalmip [37]. The identification was executed with two different regularization values $\mathbf{p}_\mathrm{reg}$. The nominal values, abbreviated as Nom, and the two regularization/initial values, referred to as RG1 and RG2, are shown in Fig. 3. The corresponding identification results are referred to as ID1 and ID2. The first set of regularization values for the rigid bodies are below the (actual) nominal values, while all values of the second regularization are above the nominal ones. It is apparent that some parameters converged toward the nominal values while some did not, e.g. the

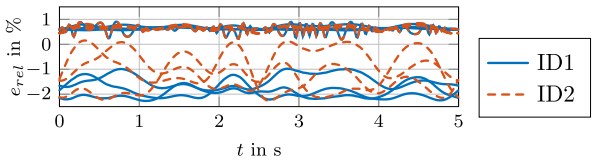

Fig. 4. Relative errors of the identified entries of the mass matrix for two different values of the regularization parameters (i.e. initial values).

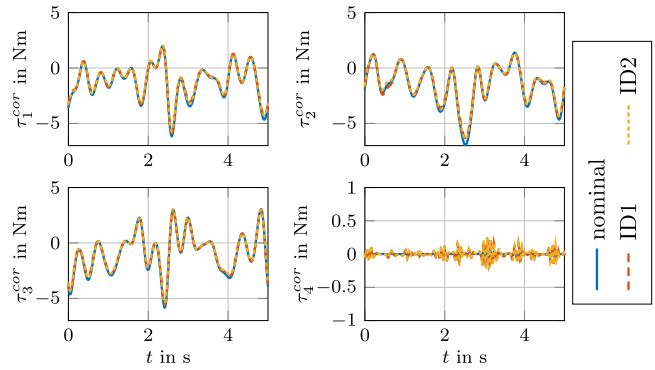

Fig. 5. Comparison of the Coriolis terms $\boldsymbol{\tau}^{\text{cor}} = \mathbf{C}(\mathbf{q}, \dot{\mathbf{q}})\dot{\mathbf{q}}$ of the nominal and the identified models with two different regularizations.

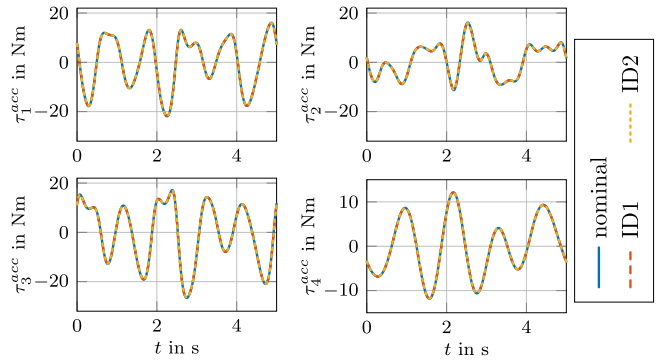

Fig. 6. Comparison of the acceleration terms $\boldsymbol{\tau}^{\text{acc}} = \mathbf{M}(\mathbf{q})\ddot{\mathbf{q}}$ of the nominal and the identified models with two different regularizations.

platform mass when using the first regularization. The nominal parameter $\mathbf{p}_v^{\mathsf{T}} = [2 \;\; 2 \;\; 2 \;\; 0.5]\,\text{Nm/(rad/s)}$, for viscous, and $\mathbf{p}_c^{\mathsf{T}} = [4 \;\; 4 \;\; 4 \;\; 1]$ in Nm, for Coulomb friction were used in the model. The relative error of the identified friction parameter is under 2.2%.

Since the inertia parameters of the simulated model are known exactly, the elements of the identified generalized mass matrix $\mathbf{M}$ can be checked against the nominal values. Denote with $\mathbf{M}_{\text{Ident}} := \mathbf{M}(\mathbf{q}, \mathbf{p}_{\text{Ident}})$ the mass matrix in terms of the identified parameters $\mathbf{p}_{\text{Ident}}$, and in terms of the nominal parameters $\mathbf{p}_{\text{Nom}}$ with $\mathbf{M}_{\text{Nom}} := \mathbf{M}(\mathbf{q}, \mathbf{p}_{\text{Nom}})$. Fig. 4 shows the relative errors $\mathbf{e}_{rel} = \frac{\mathbf{M}_{\text{Nom}}(i,j) - \mathbf{M}_{\text{Ident}}(i,j)}{\text{mean}(\mathbf{M}_{\text{Nom}}(i,j))}$ of the 6 elements of the respective identified mass matrix along the trajectory. The relative errors of the main diagonal elements are below 1%, those of the off-diagonal elements are about 2%. Fig. 5 shows the torque $\boldsymbol{\tau}^{\text{cor}} = \mathbf{C}(\mathbf{q}, \dot{\mathbf{q}})\dot{\mathbf{q}}$ due to the Coriolis/centrifugal effects, whereas Fig. 6 depicts the torque $\boldsymbol{\tau}^{\text{acc}} = \mathbf{M}(\mathbf{q})\ddot{\mathbf{q}}$ for the nominal and the identified model when using the two different regularization values as initial guess. The difference of identified and the nominal torque is less than 1% at any time. The identified mass matrix was positive definite along the trajectory, which was checked by application of the Cholesky factorization. The identification was carried out for several different regularization values. The results were always similar. By construction, the obtained parameters are physically consistent and $\mathbf{M}$ positive definite.

VIII. Example 2: Industrial Delta Robot

The proposed identification is applied to the ABB IRB 360-6/1600 Delta robot. Coulomb and viscous friction are modeled for the four actuated joints. The prismatic joint in the telescope bar shows significant friction, hence viscous and Coulomb friction are also modeled for this joint.

A. Regularization Using Estimated Parameters

The regularization values $\mathbf{p}_{\text{reg}}$, which are used as initial values for the identification, are helpful for speeding up the optimization. For most industrial robots no reliable CAD data is available (e.g. no volumetric information). Regularization terms are therefore obtained from geometric approximations.

The upper arms can be approximated as hollow cylinders of carbon fiber. The length ($500\,\text{mm}$) and wall thickness ($3\,\text{mm}$) for the carbon fiber part is assumed to calculate the mass and the first and second inertia moments w.r.t. the link frame. The longitudinal and lateral inertia are computed as $\frac{1}{2}m(R_o^2 + R_i^2)$ and $\frac{1}{12}m(L^2 + 3(R_o^2 + R_i^2))$, where m denotes the mass, L the length and R_o, R_i the outer and inner radii, respectively. Analogously the regularization values for the struts are obtained using the length $1106\,\text{mm}$, assumed wall thickness of $1\,\text{mm}$ and the COM to be in the middle of the carbon fiber part. The two ball sockets at both ends of the struts weigh roughly the same as the carbon fiber part, so these two sockets are similarly assumed as hollow cylinders and accounted for in the regularization term for the struts. The same approximation is used to obtain initial guesses for the telescope bar with the assumption that the upper part (length $700\,\text{mm}$, radius $8\,\text{mm}$) is $\frac{6}{10}m$ of the complete telescope bar and assumed to be a steel cylinder, whereas the lower part (length $780\,\text{mm}$, outer radius $14\,\text{mm}$, inner radius $8\,\text{mm}$) as a hollow synthetic material cylinder with $\frac{4}{10}m$. For the upper part of the telescope bar the simplified formula for the inertia w.r.t. the link for a slender strut can be applied, whereas for the lower part the same approximation with a hollow cylinder is possible. Since the telescope bar cannot be disassembled, no further insight of the assembled parts is possible. The mass of the moving platform can be obtained by approximation as two cylinders of aluminum.

B. Dynamic Parameter Identification

The objective function $J(\boldsymbol{\pi})$ in (15) is minimized, where initial values are obtained as $\boldsymbol{\pi}_0 = \arg\min_{\boldsymbol{\pi}} \;\; \|\mathbf{p} - \mathbf{p}_{\text{reg}}(\boldsymbol{\pi})\|_2^2$ with regularization parameters $\mathbf{p}_{\text{reg}}$ obtained in Section VII-I-A. Table I shows the parameters of the upper arms, struts, platform, and telescope bar obtained with the two different regularizations/initial guesses, referred to as RG simple and RG geom. One regularization was obtained by a simple guess

TABLE I
IDENTIFIED NON-ZERO PARAMETER OF THE INDUSTRIAL DELTA ROBOT

Param.	RG simple	ID simple	RG geom	ID geom	Unit
Upper Arm					
$m\,c_y$	0.250	0.128	0.101	0.091	$\mathrm{kg\,m}$
$m\,c_z$	0.000	-0.090	0.000	0.009	$\mathrm{kg\,m}$
Θ_{yy}	0.084	0.146	0.127	0.189	$\mathrm{kg\,m^2}$
Strut					
m	0.200	0.250	0.249	0.278	kg
$m\,c_x$	0.111	0.072	0.129	0.104	$\mathrm{kg\,m}$
Θ_{xx}	0.003	17.446	0.032	24.611	$10^{-3}\mathrm{kg\,m^2}$
Θ_{yy}	0.082	0.086	0.109	0.114	$\mathrm{kg\,m^2}$
Θ_{zz}	0.082	0.089	0.109	0.116	$\mathrm{kg\,m^2}$
Platform					
m	0.800	1.008	1.000	1.230	kg
Telescope Bar (upper part)					
m	0.900	0.901	0.900	0.732	kg
$m\,c_x$	-0.315	-0.100	-0.315	-0.305	$\mathrm{kg\,m}$
Θ_{xx}	0.147	0.168	0.147	0.148	$\mathrm{kg\,m^2}$
Θ_{yy}	0.147	0.168	0.147	0.148	$\mathrm{kg\,m^2}$
Θ_{zz}	28.800	0.884	28.800	2.826	$10^{-6}\,\mathrm{kg\,m^2}$
Telescope Bar (lower part)					
m	0.600	0.456	0.600	0.483	kg
$m\,c_x$	0.234	0.251	0.234	0.239	$\mathrm{kg\,m}$
Θ_{xx}	0.122	0.141	0.122	0.126	$\mathrm{kg\,m^2}$
Θ_{yy}	0.122	0.141	0.122	0.126	$\mathrm{kg\,m^2}$
Θ_{zz}	78.000	0.010	78.000	1.151	$10^{-6}\mathrm{kg\,m^2}$

and the other by taking into account the geometry with assumed materials. The obtained parameters for the strut remain close to the initial value for both regularizations. The identified mass of the platform increased by roughly 20% for both regularizations. In case of the upper arms, there is also a noticeable difference. Comparison of these results shows, that for both regularization the mass of the struts and platform increased, whereas the mass of the lower part of the telescope bar decreased. Both results lead to physically consistent bodies, and hence a positive definite and symmetric mass matrix $\mathbf{M}(\mathbf{q}, \mathbf{p}_{\mathrm{Ident}})$. The identified lumped inertia of the fourth motor is $\Theta = 2.87 \times 10^{-3}\ \mathrm{kg\,m^2}$. The obtained friction parameters for the drives are $\mathbf{p}_v = [1.576 \quad 1.667 \quad 1.411 \quad 0.019]$ in $\mathrm{Nm}/\frac{\mathrm{rad}}{\mathrm{s}}$ and $\mathbf{p}_c = [4.659 \quad 4.644 \quad 6.353 \quad 0.807]$ in Nm. The friction coefficients for the prismatic joint of the telescope bar are $p_v = 4.08\ \mathrm{N}/\frac{\mathrm{m}}{\mathrm{s}}$ and $p_c = 5.36\,\mathrm{N}$.

C. Inverse Dynamics Verification

To validate the identification results, a different trajectory is used, for which the joint torques $\boldsymbol{\tau}$ are recorded. This verification trajectory is obtained as another excitation trajectory by optimizing it with different start values for the coefficients $\mathbf{a}$ and $\mathbf{b}$. The results for the drive torques $\boldsymbol{\tau} = \mathbf{Y}(\mathbf{q}, \dot{\mathbf{q}}, \ddot{\mathbf{q}})\,\mathbf{p}_{\mathrm{Ident}} = \mathbf{M}(\mathbf{q})\ddot{\mathbf{q}} + \mathbf{C}(\mathbf{q}, \dot{\mathbf{q}})\dot{\mathbf{q}} + \mathbf{g}(\mathbf{q}) + \mathbf{f}(\dot{\mathbf{q}})$, when executing the verification trajectory, are shown in Fig. 7. The first three torques fit well while the result for the spindle torque τ_4 is not satisfactory, for the base-parameter method as well as the proposed method. The simple friction model was identified as reason for the relatively large error. The maximal speed of the identification trajectory was $\max(|\dot{q}_4|) \approx 2760\,^\circ/\mathrm{s}$, and maximal acceleration was $\max(|\ddot{q}_4|) \approx 13.8 \times 10^3\,^\circ/\mathrm{s}^2$, whereas the verification trajectory had a maximal velocity $\max(|\dot{q}_4|) \approx 175\,^\circ/\mathrm{s}$ and acceleration $\max(|\ddot{q}_4|) \approx 500\,^\circ/\mathrm{s}^2$. Changing the viscous friction coefficient of the actuated joint 4 to five times of the identified value, and decreasing the Coulomb coefficient by factor 0.75,

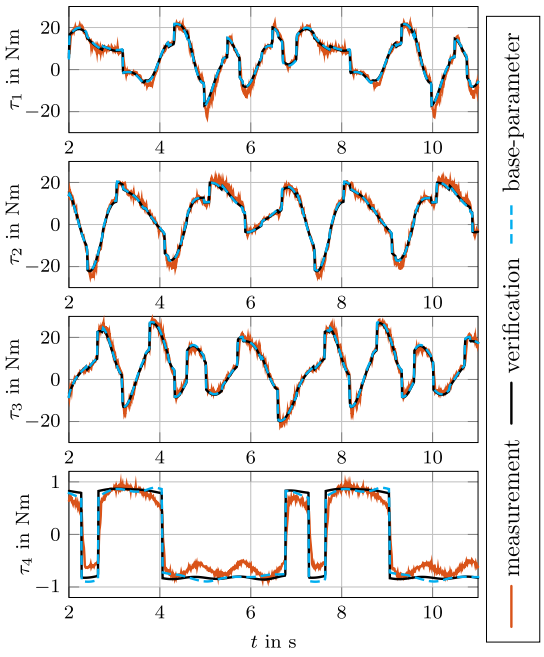

Fig. 7. Motor torques $\boldsymbol{\tau}$ for the verification trajectory. The root mean squared (RMS) error of the base-parameter identification $\mathbf{e}_{\mathrm{RMS}}(\mathbf{p}_{\mathrm{B}}) = [2.0 \quad 1.8 \quad 2.2 \quad 0.25]\,\mathrm{Nm}$ is close to the $\mathbf{e}_{\mathrm{RMS}}(\mathbf{p}_{\mathrm{Ident}}) = [2.0 \quad 1.7 \quad 2.2 \quad 0.20]\,\mathrm{Nm}$ of the parameter $\mathbf{p}_{\mathrm{Ident}}$ identified with the proposed method.

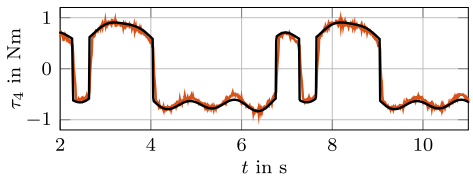

Fig. 8. Verification with changed parameters for the viscous and Coulomb friction of the fourth drive. This yields a RMS error $e_{\mathrm{RMS}} = 0.15\,\mathrm{Nm}$.

yields the result in Fig. 8. It is concluded that an improved friction model is required if the full speed range of the fourth drive is to be covered.

IX. CONCLUSION

A method to identify physically consistent dynamics parameters for the family of Delta robots was presented. It was applied to a surrogate test model (simulation) with known parameters, and to a real industrial 4 DOF Delta robot. The approach makes use of a generic model that satisfies certain model simplifications, such as omitting negligible or non-excited inertia parameter. The method is does not need CAD data or data provided by the robot manufacturer. These simplifications can be relaxed if data on the dynamics parameters becomes available. All necessary conditions for physical consistency are encoded in the non-linear parameter transformation (14), such that efficient unconstrained optimization methods can be applied for solving the identification problem (15). The identical limbs and kinematical structure of the Delta robot allowed to systematically reduce the number of variables needed to express the required inertia parameters, and hence improve the identification result. The problem that not all inertia parameters are identifiable, which motivated the standard base-parameter method, is tackled by prescribing regularization

values. The latter are a means to obtain dynamic parameters close to certain parameter values for which reliable estimates exist. Results for the simulation model show that the mass matrix, forces due to acceleration, the Coriolis and centrifugal, gravitation, and friction forces are well approximated by the identified model.

The presented method ensures that every rigid body is physically consistent, thus the model (1) is physically consistent, in particular the generalized mass matrix $\mathbf{M}$ is guaranteed to be positive definite and symmetric. This provides the basis for forward dynamics simulations and advanced model-based control schemes with realistically identified dynamic parameters.

Future work will address means to identify the correct (in addition to physically consistent) values of mass-inertia parameters of each individual body using additional data such as force measurements. This is a precondition for model-based control when joint reaction forces are to be limited [38]. The latter is important for many realizations of Delta robots.

REFERENCES

[1] H. Khalil, *Nonlinear Systems*. Hoboken, NJ, USA: Prentice Hall, 2002.

[2] R. Ortega and E. García-Canseco, "Interconnection and damping assignment passivity-based control: A survey," *Eur. J. Control*, vol. 10, no. 5, pp. 432–450, 2004.

[3] R. Kelly and R. Carelli, "A class of nonlinear PD-Type controllers for robot manipulators," *J. Robotic Syst.*, vol. 13, no. 12, pp. 793–802, 1996.

[4] W. Khalil and E. Dombre, *Modeling, Identification and Control of Robots*. Oxford, U.K.: Butterworth-Heinemann, 2004.

[5] H. Abdellatif, M. Grotjahn, and B. Heimann, "Independent identification of friction characteristics for parallel manipulators," *J. Dynamic Syst. Meas. Control*, vol. 129, no. 3, pp. 294–302, 2006.

[6] V. Nabat, O. Company, F. Pierrot, and P. Poignet, "Dynamic modeling and identification of Par4, a very high speed parallel manipulator," in *Proc. IEEE/RSJ Int. Conf. Intell. Robots Syst.*, 2006, pp. 496–501.

[7] K. Yoshida, K. Osuka, H. Mayeda, and T. Ono, "When is the set of base-parameter values physically impossible?," *J. Robot. Soc. Jpn.*, vol. 14, no. 1, pp. 122–130, 1996.

[8] K. Yoshida and W. Khalil, "Verification of the positive definiteness of the inertial matrix of manipulators using base inertial parameters," *Int. J. Robot. Res.*, vol. 19, no. 5, pp. 498–510, 2000.

[9] C. D. Sousa and R. Cortesão, "Physical feasibility of robot base inertial parameter identification: A linear matrix inequality approach," *Int. J. Robot. Res.*, vol. 33, no. 6, pp. 931–944, 2014.

[10] S. Traversaro, S. Brossette, A. Escande, and F. Nori, "Identification of fully physical consistent inertial parameters using optimization on manifolds," in *Proc. IEEE/RSJ Int. Conf. Intell. Robots Syst.*, 2016, pp. 5446–5451.

[11] P. M. Wensing, S. Kim, and J.-J. Slotine, "Linear matrix inequalities for physically-consistent inertial parameter identification: A statistical perspective on the mass distribution," *IEEE Robot. Automat. Lett.*, vol. 3, no. 1, pp. 60–67, Jan. 2018.

[12] C. D. Sousa and R. Cortesão, "Inertia tensor properties in robot dynamics identification: A linear matrix inequality approach," *IEEE/ASME Trans. Mechatronics*, vol. 24, no. 1, pp. 406–411, Feb. 2019.

[13] C. Rucker and P. M. Wensing, "Smooth parameterization of rigid-body inertia," *IEEE Robot. Automat. Lett.*, vol. 7, no. 2, pp. 2771–2778, Apr. 2022.

[14] J. M. E. Hernandez, A. Chemori, and H. A. Sierra, *Modeling and Nonlinear Robust Control of Delta-Like Parallel Kinematic Manipulators*. Amsterdam, The Netherlands: Elsevier, 2022.

[15] R. Clavel, "Delta, a fast robot with parallel geometry," in *Proc. 18th Int. Symp. Ind. Robots*, 1988, pp. 91–100.

[16] F. Pierrot and O. Company, "H4: A new family of 4-DOF parallel robots," in *Proc. IEEE/ASME Int. Conf. Adv. Intell. Mechatronics*, 1999, pp. 508–513.

[17] S. Krut, M. Benoit, H. Ota, and F. Pierrot, "I4: A new parallel mechanism for Scara motions," in *Proc. IEEE Int. Conf. Robot. Automat.*, 2003, pp. 1875–1880.

[18] F. Pierrot, V. Nabat, O. Company, S. Krut, and P. Poignet, "Optimal design of a 4-DOF parallel manipulator: From academia to industry," *IEEE Trans. Robot.*, vol. 25, no. 2, pp. 213–224, Apr. 2009.

[19] F. Falezza et al., "Gray-box model identification and payload estimation for delta robots," *IFAC-PapersOnLine*, vol. 53, no. 2, pp. 8771–8776, 2020.

[20] T.-H. Kim, Y. Kim, T. Kwak, and M. Kanno, "Metaheuristic identification for an analytic dynamic model of a delta robot with experimental verification," *Actuators*, vol. 11, no. 12, 2022, Art. no. 352.

[21] C. Baradat, V. Nabat, S. Krut, and F. Pierrot, "Par2: A spatial mechanism for fast planar, 2-DoF, pick-and-place applications," in *Proc. Second Int. Workshop Fundam. Issues Future Res. Directions Parallel Mechanisms Manipulators*, 2009.

[22] A. Vivas, P. Poignet, F. Marquet, F. Pierrot, and M. Gautier, "Experimental dynamic identification of a fully parallel robot," in *Proc. IEEE Int. Conf. Robot. Automat.*, 2003, pp. 3278–3283.

[23] P. Renaud et al., "Kinematic and dynamic identification of parallel mechanisms," *Control Eng. Pract.*, vol. 14, no. 9, pp. 1099–1109, 2006.

[24] M. Díaz-Rodríguez, Á. Valera, V. Mata, and M. Valles, "Model-based control of a 3-DOF parallel robot based on identified relevant parameters," *IEEE/ASME Trans. Mechatronics*, vol. 18, no. 6, pp. 1737–1744, Dec. 2013.

[25] M. Díaz-Rodríguez, V. Mata, Á. Valera, and Á. Page, "A methodology for dynamic parameters identification of 3-DOF parallel robots in terms of relevant parameters," *Mechanism Mach. Theory*, vol. 45, no. 9, pp. 1337–1356, 2010.

[26] S. Briot, S. Krut, and M. Gautier, "Dynamic parameter identification of over-actuated parallel robots," *J. Dynamic Syst. Meas. Control*, vol. 137, no. 11, 2015, Art. no. 111002.

[27] A. Rosyid and B. El-Khasawneh, "Identification of the dynamic parameters of a parallel kinematics mechanism with prismatic joints by considering varying friction," *Appl. Sci.*, vol. 10, 2020, Art. no. 4820.

[28] J. P. Norton, *An Introduction to Identification*. Cambridge, MA, USA: Academic Press, 1986.

[29] S. M. Kay, *Fundamentals of Statistical Signal Processing, Volume I: Estimation Theory*. Hoboken, NJ, USA: Prentice-Hall, 1993.

[30] J. Swevers, W. Verdonck, and J. D. Schutter, "Dynamic model identification for industrial robots," *IEEE Control Syst. Mag.*, vol. 27, no. 5, pp. 58–71, Oct. 2007.

[31] M. Gautier and W. Khalil, "Exciting trajectories for the identification of base inertial parameters of robots," in *Proc. IEEE Conf. Decis. Control*, 1991, pp. 494–499.

[32] T. Lee, B. D. Lee, and F. C. Park, "Optimal excitation trajectories for mechanical systems identification," *Automatica*, vol. 131, 2021, Art. no. 109773.

[33] J. J. Uicker, B. Ravani, and P. N. Sheth, *Matrix Methods in the Design Analysis of Mechanisms and Multibody Systems*. New York, NY, USA: Cambridge Univ. Press, 2013.

[34] J. G. Papastavridis, *Analytical Mechanics*. Singapore: World Sci., 2014.

[35] T. Lee and F. C. Park, "A geometric algorithm for robust multibody inertial parameter identification," *IEEE Robot. Automat. Lett.*, vol. 3, no. 3, pp. 2455–2462, Jul. 2018.

[36] T. Lee, P. M. Wensing, and F. C. Park, "Geometric robot dynamic identification: A convex programming approach," *IEEE Trans. Robot.*, vol. 36, no. 2, pp. 348–365, Apr. 2020.

[37] J. Lofberg, "YALMIP: A toolbox for modeling and optimization in MATLAB," in *Proc. IEEE Int. Conf. Robot. Automat.*, 2004, pp. 284–289.

[38] D. Gnad, H. Gattringer, A. Müller, W. Höbarth, R. Riepl, and L. Messner, "Computation of dynamic joint reaction forces of PKM and its use for load-minimizing trajectory planning," in *Proc. IEEE Int. Conf. Robot. Automat.*, 2022, pp. 4848–4854.